Journal of Materials Chemistry A

Accepted Manuscript

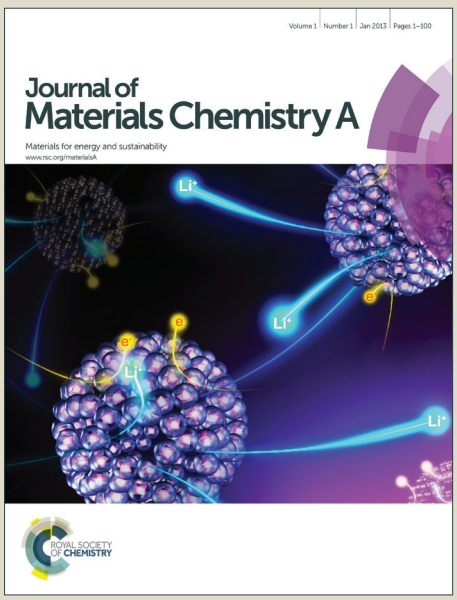

ROYAL SOCIETY OF CHEMISTRY

www.rsc.org/materialsA

Cite this: DOI: 10.1039/c0xx00000x

www.rsc.org/xxxxxx

ARTICLE TYPE

Low Temperature Preparation of TiO_2 Nanoparticle Chains without Hydrothermal Treatment for Highly Efficient Dye-Sensitized Solar Cells

Yan Cui, Lu Zhang, Kai Lv, Gang Zhou, and Zhong-Sheng Wang*

Received (in XXX, XXX) Xth XXXXXXXXX 20XX, Accepted Xth XXXXXXXXX 20XX
DOI: 10.1039/b000000x

Nanoparticle chains of anatase TiO_2 composed of ~5 nm nanoparticles with high surface area (309 m^2 g^{-1}) are prepared by slow hydrolysis of titanium tetraisopropoxide modified with glacial acetic acid at a temperature of 50 °C. These nanoparticle chains without hydrothermal treatment can be used directly to fabricate photoanodes for highly efficient dye-sensitized solar cells (DSSCs), which achieves power conversion efficiency of 9.80% at simulated AM1.5G illumination (100 mW cm^{-2}). The approach presented in this study demonstrates a facial synthesis of anatase TiO_2 chains for use in DSSCs, which avoids hazards arising from a hydrothermal process that is typically adopted to prepare crystalline TiO_2 nanoparticles as the photoanode in DSSCs.

Introduction

Dye-sensitized solar cells (DSSCs)[1] are promising photovoltaic devices owing to their low-cost and high efficiency.[2] Nanocrystalline TiO_2 is the state-of-the-art photoanode material for a DSSC to perform efficiently. The specific surface area, crystal phase, crystallinity and morphology for the TiO_2 NPs (NPs) play important roles in solar cell performance.[3-8] Anatase TiO_2 NPs with both high surface area, good crystallinity and suitable pore size is desired for high-performance DSSCs.

The performance of DSSCs depends on the particle size, pore size, and charge transport properties of the titania NP photoanode.[9-11] According to the established results,[9,10] smaller NPs have higher surface area but shorter electron diffusion length and poor light scattering ability, while larger NPs have longer electron diffusion length and higher light scattering ability but lower surface area. For this reason, there is an optimal particle size for best efficiency. For example, Cao et al. concluded that 15 nm NP was best among the 10 nm, 15 nm, 20 nm samples,[9] and Yang et al. found that long-thin nanorods (120 nm long, 17 nm wide) were better than the short-thin (50 nm long, 15 nm wide) and long-thick (150 nm long, 25 nm wide) nanorods in terms of photovoltaic performance.[10] The optimal size seems to depend on the morphology of NP.

The reported titania NPs used in efficient DSSCs are usually prepared with a sol-gel process followed by hydrothermal treatment.[8-11] However, the hydrothermal treatment leads to prominent particle growth, which significantly reduces surface area and hence dye loading. Furthermore, the hydrothermal treatment is hazardous and energy consuming, which should be avoided in a large-scale production. To avoid hazards and meanwhile enhance surface area, it is necessary to develop a mild synthetic method for anatase TiO_2 NPs with both good crystallinity and high surface area.

Tiny NPs can be easily obtained from a sol-gel process, but it is unsuccessful to use the sol-gel titania NPs for fabrication of high quality titania films due to the poor crystallinity or amorphous feature. Although thermal annealing during film fabrication is able to induce crystallization of amorphous NPs, the film is easy to crack and drop off from the substrate, limiting its use in DSSCs. It thus remains a big challenge to develop well-crystallized sol-gel NPs without hydrothermal treatment so that they can form robust films with strong adhesion to the substrate. Herein, we report a facial synthesis of TiO_2 NP chains through a slow hydrolysis of titanium tetraisopropoxide (TTIP) at 50 °C in the presence of large amount of glacial acetic acid. NP chains composed of tiny NPs (~5 nm in diameter) are obtained, which have good crystallinity in anatase phase without subsequent hydrothermal or sintering treatment and can form crack-free films on the conductive substrate for use as photoanode in high-performance DSSCs. The as-synthesized NP chains have surface area as high as 309 m^2 g^{-1}, which guarantees high dye loading for efficient light harvesting. Moreover, the interconnection of NPs in the chain is expected to improve electron diffusion length, which is an important factor influencing solar cell performance. When applied as the photoanode in DSSCs, the power conversion efficiency (PCE) of 9.80% is achieved, with short-circuit photocurrent (J_{sc}) of 15.67 mA cm^{-2}, open-circuit photovoltage (V_{oc}) of 812 mV, and fill factor (FF) of 0.77. Our method is different from the reported methods[8-11] in particle shape and hydrothermal treatment. In particular, it is successful to get well crystallized NP chains using a low temperature sol-gel process without hydrothermal treatment for use as efficient photoanode in highly efficient DSSCs for the first time, to the best of our knowledge.

Results and Discussion

The TiO_2 NPs were prepared from the hydrolysis of TTIP mixed with large amount of glacial acetic acid (HAc) at 50 °C, as

detailed in the Experimental Section. The presence of large amount of acetic acid acted as a chemical modifier of TTIP, which slowed down the hydrolysis of TTIP when water was introduced, because acetate is less hydrolysable than isopropoxy. The formed gel was very stable without sedimentation for long time storage. This means that the as prepared titania is water soluble and very stable in the presence of HAc.

Figure 1a illustrates the X-ray diffraction (XRD) pattern of the as-prepared TiO_2 powder dried at room temperature. The observed XRD peaks presented in Figure 1a are attributed to anatase TiO_2 (JCPDS No. 21-1272). The clear observation of strong anatase XRD peaks is indicative of good crystallinity for the as-prepared TiO_2 NPs. The average nanocrystal size is calculated to be 5.3 nm based on the Scherrer equation from the strongest diffraction peak (101). As compared to the standard XRD patterns, the (004) peak is comparatively stronger while the (200) peak is comparatively weaker. Such features suggest the formation of rod-like nanocrystals with a preferred growth orientation along the *c*-axis of the anatase lattice.[12]

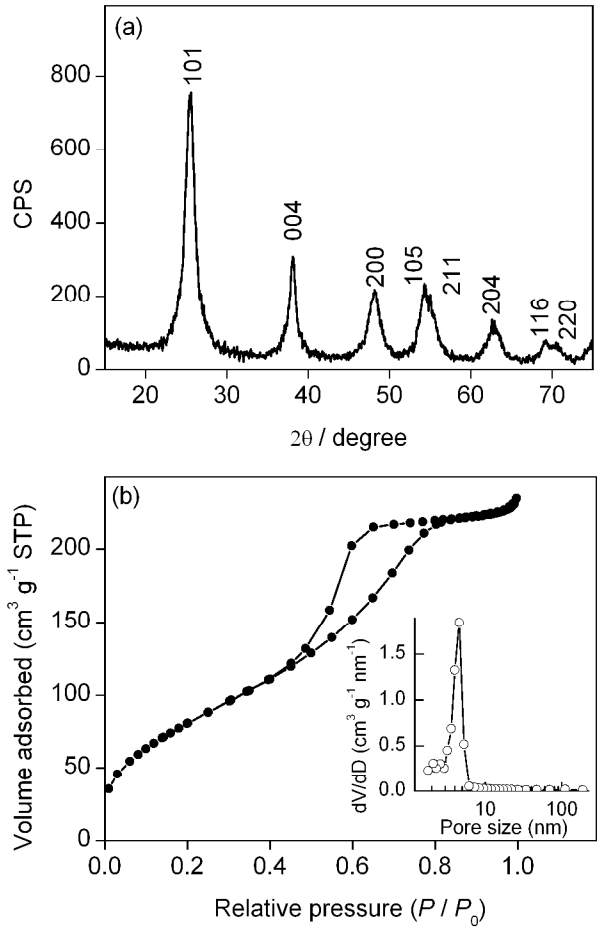

Figure 1. XPD pattern (a) and nitrogen sorption isotherm (b) for the as-prepared TiO_2 NP chains. Inset in b is the pore size distribution.

According to the reported methods,[10,11] NPs directly obtained from a sol-gel reaction system containing 0.1 M acid or base are usually amorphous or poorly crystallized without hydrothermal treatment, and the XRD pattern is almost featureless, because hydrolysis and condensation are very fast and proceed immediately. However, when large amount of HAc is first mixed with TTIP, the hydrolysis and condensation become slower, promoting crystallization of NPs at low temperature. The presence of large amount of HAc promotes polycondensation, leading to extensive Ti-O-Ti network.[12]

The specific surface area and pore size distribution of the as-prepared TiO_2 were characterized using nitrogen gas sorption. The type IV isotherm and H1 type hysteresis loop were observed for the as-prepared TiO_2 (Figure 1b), suggesting the product that was mesoporous. The specific surface area, calculated with the standard multi-points Brunauer-Emmett-Teller (BET) method, was 309 m^2 g^{-1}, much larger than that of the 25-nm NPs.[13] The as-prepared sample shows a narrow pore size distribution centered at 5 nm (inset of Figure 1b), revealing a homogenous pore size in the sample. Such a high surface area is advantageous to adsorb large amount of dye molecules, which is favourable for enhancing light harvesting efficiency and hence photocurrent of DSSCs.

The transmission electronic microscopy (TEM) image for the as-prepared TiO_2 NPs is shown in Figure 2a. The diameter of the particle is determined of ~5 nm, being consistent with the results calculated from the XRD and BET data. Small NPs of ~5 nm in size are partially fused and interconnected together, forming a network of NP chains (Figure 2a and its magnified picture in Figure S1). High-resolution TEM image (Figure 2b) reveals the single crystal nature of such NP chains. Interplanar distances obtained from the lattice fringe correspond to the (101), (004) and (200) crystal planes of anatase TiO_2. This further confirms the preferred growth orientation of NP chains along the *c*-axis of the anatase lattice as observed in the XRD profile (Figure 1a).

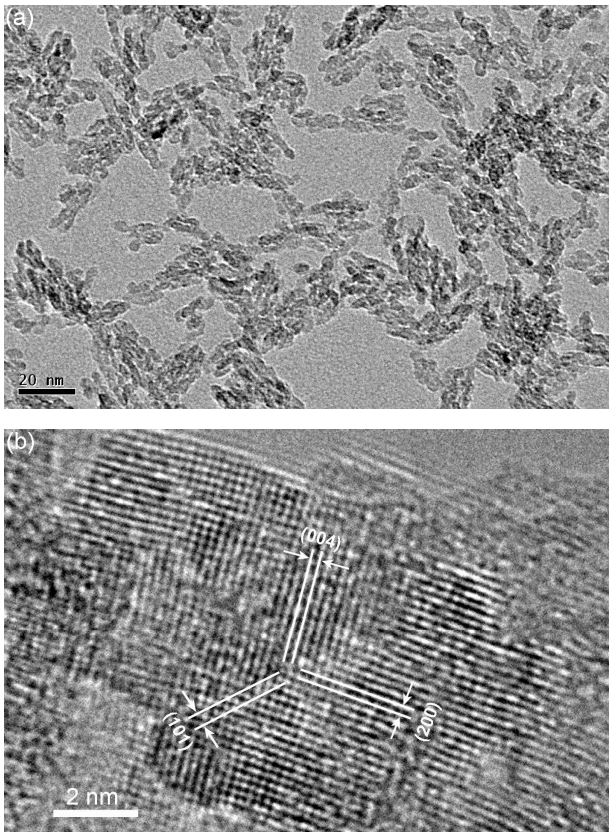

Figure 2. TEM (a) and HRTEM (b) of the as-prepared TiO_2 NP chains.

As the titania film should be sintered at 500 ^{o}C for 2 h in the fabrication of DSSCs, it is necessary to examine the TEM images of the sintered sample. As shown in Figure 3, long NP chains (hundreds of nm long) are connected by small NPs. This indicates that NP chains still exist in the sintered sample. Partial fusion of adjacent NPs makes the chain boundary-free. The sintering at 500 ^{o}C for 2 h resulted in an increase in particle size from 5 to 10 nm and an increase in pore diameter from 5 to 8 nm. The BET surface area decreased significantly to 160 m^2 g^{-1}, which is still much higher than that (60 m^2 g^{-1}) for the 25-nm NPs.[13]

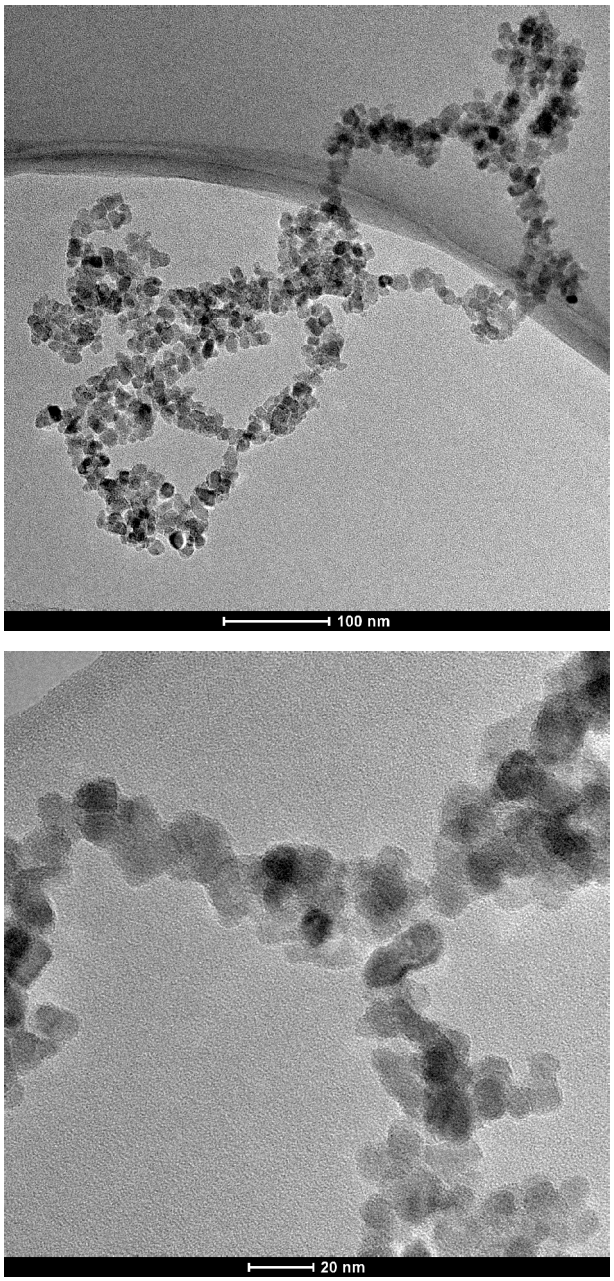

Figure 3. TEM images with different magnifications for the NP chains sintered at 500^{o}C for 2 h

Yang and co-workers prepared similar TiO_2 nanorods connected by several primary crystallites.[10] As compared with their method,[10] this approach is more simple, safer and lower energy-consuming. In particular, the synthesized NP chains are soluble and have good crystallinity even though hydrothermal treatment or sintering is not applied to the system.

The as-prepared TiO_2 NP chains were used to fabricate TiO_2 films with various thicknesses, which were sintered at 500 ^{o}C for 2 h to remove the organic binder. The films were sensitized with cis-bis(isothiocyanato) bis(2,2'-bipyridyl-4,4'-dicarboxylato) ruthenium(II) tetrabutylammonium (the so-called N719, Solaronix SA). Figure 4a displays the incident monochromatic photon-to-electron conversion efficiency (IPCE) as a function of wavelength for the fabricated DSSCs. The maximum IPCE value at 530 nm increased gradually with film thickness up to 13.9 μm due to the increased dye loading, and then changed negligibly from 13.9 to 16.5 μm. Taking the light absorption and reflection of the substrate into account, the obtained IPCE value of ~90% at 530 nm represent a unity photon-to-electron conversion for the film thickness from 13.9 to 16.5 μm. Furthermore, the IPCE spectrum becomes broadened with film thickness, which is attributed to the increased dye loading. The integrated photocurrents were calculated from the IPCE spectra (Figure 4a) and the standard AM1.5G solar emission spectrum, as summarized in Table 1. It is judged from the IPCE spectra that the best film thickness falls in the range of 13.9 to 16.5 μm for efficient photoelectric conversion in a broad spectral range. The best range of film thickness is expected to generate the highest photocurrent at simulated AM1.5G solar illumination as predicted from the trend of integrated photocurrent with film thickness (Table 1).

The performance of above DSSCs was tested under illumination of simulated AM1.5G solar light (100 mW cm^{-2}), and the current-voltage characteristics are shown in Figure 4b for each individual cell. The relationship between average photovoltaic performance parameters and film thickness is summarized in Table 1. With increasing the film thickness, J_{sc} increased with film thickness up to 13.9 μm, and then hardly changed with further increasing the film thickness up to 16.5 μm. The trend of J_{sc} was consistent with that of the integrated photocurrents. However, the measured J_{sc} was lower than the corresponding integrated photocurrent by about 10% for each thickness. The small pore size (8 nm for the sintered sample) of the NP chain film slowed down the diffusion of I_3^-/I^- ions so that photocurrent generation under full sun illumination was limited by diffusion kinetics. However, under illumination of lower light intensity for IPCE measurement, much fewer dye molecules were active, and the diffusion of I_3^-/I^- ions was fast enough to completely regenerate dye molecules. As a consequence, the integrated photocurrent was higher than the measured J_{sc}.

Cite this: DOI: 10.1039/c0xx00000x

www.rsc.org/xxxxxx

ARTICLE TYPE

Table 1. Integrated photocurrents and measured photovoltaic performance parameters at simulated AM1.5G solar light (100 mW cm^{-2})[a]

Thickness (μm)	J_{int} (mA cm^{-2})	J_{sc} (mA cm^{-2})	V_{oc} (mV)	*FF*	*PCE* (%)
5.5	10.83±0.15	9.91±0.27	837±12	0.76±0.00	6.31±0.32
8.3	14.00±0.06	12.77±0.06	815±3	0.76±0.00	7.97±0.07
11.1	14.95±0.17	13.39±0.07	799±19	0.76±0.00	8.34±0.12
13.9	16.51±0.06	15.34±0.07	773±9	0.76±0.01	8.96±0.04
16.5	17.03±0.25	15.41±0.21	764±3	0.76±0.01	9.01±0.27

[a] J_{int} is the integrated photocurrent, and the other parameters are obtained from measurements at simulated AM1.5G solar light (100 mW cm^{-2}). Four parallel cells were measured for each film thickness.

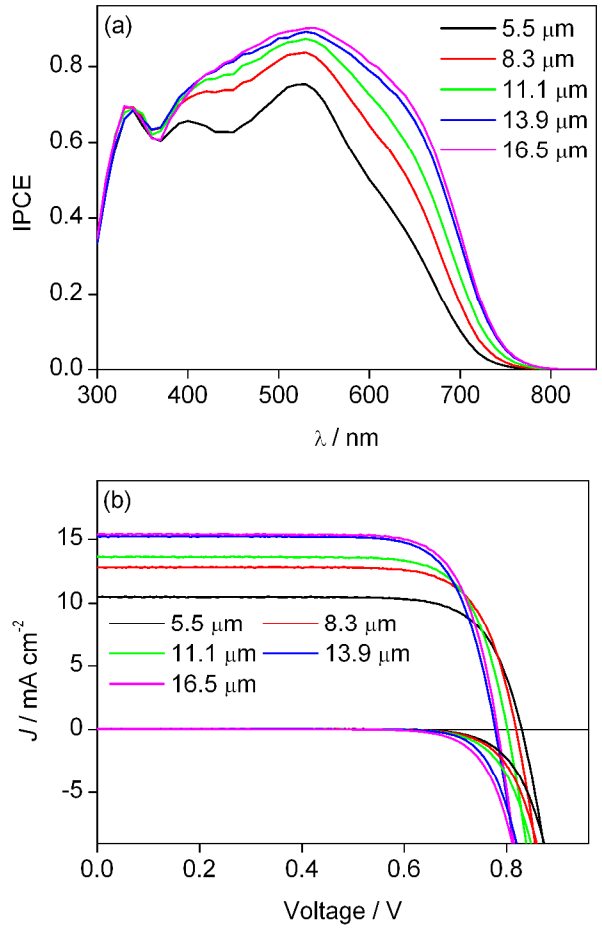

Figure 4. IPCE spectra (a) and current-voltage curves (b) for the DSSCs with different film thicknesses

The overall trend of V_{oc} was decreasing with film thickness. As charge recombination speeded up with film thickness as evidenced by the gradual shift of dark current onset potential to larger value (Figure 4b), the increased voltage loss resulting from the increased charge recombination rate led to a decrease in V_{oc}. By contrast, FF showed negligible change in the film thickness range from 5.5 to 16.5 μm. As a consequence, PCE increased with film thickness up to 13.9 μm and remained similar with further increasing the film thickness up to 16.5 μm. Based on the relationship of photovoltaic performance with film thickness, the best film thickness was also determined in the range of 13.9 to 16.5 μm for high PCE.

According to the above results, we fabricated another batch of TiO_2 films in the thickness range of 13.9 to 16.5 μm for the purpose of achieving higher efficiency, and the best cell at 15.6 μm achieved PCE of 9.80% with 15.67 mA cm^{-2} of J_{sc}, 812 mV of V_{oc}, and 0.77 of FF (Figure S2). It is noted that the best data from this batch of films was not included in Table 1 for statistics because of different thickness and different batch of films prepared at different date. For comparison, control DSSCs were fabricated using the 25-nm separated NPs obtained from a typical hydrothermal treatment.[13] Under the comparable conditions (same dye bath, same electrolyte and fabrication at the same date), the best control DSSC (~17.2 μm thick) produced PCE of 7.69% (J_{sc} = 14.72 mA cm^{-2}, V_{oc} = 736 mV, FF = 0.71), which is much lower than that for the DSSC based on these NP chains (Figure S2). Evidently, the NP chains generated much higher J_{sc} under the comparable conditions, which is attributed to the higher dye loading arising from the higher specific surface area. Because of the higher surface area, the dye amount on 5-nm NP chain film was 2-fold that on the 25-nm NP film with the same thickness (1 μm), as seen in Figure S3. Although the pore size (8 nm for the sintered sample) is small, it seems that the pore size is big enough for efficient dye adsorption as revealed by the UV-vis absorption spectra (Figure S3).

Owing to the high surface area, the NP chains based DSSC could generate PCE of 8% using 8-μm thick film, which is a high efficiency for such a thin film. High surface concentration of dye molecules is particularly advantageous to enhance light harvesting efficiency and IPCE in the long wavelength region, where extinction coefficients are low and decrease gradually with wavelength.[8] Therefore, the DSSC with the NP chains produced much higher IPCE (Figure S4a) particularly in the longer wavelength region (Figure S4b) and exhibited more broadened IPCE profile than the 25-nm NPs.

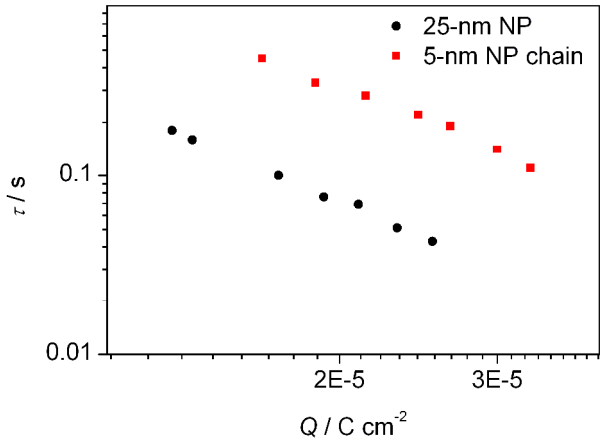

Figure 5. Electron lifetime against charge density

In addition to the important influence of surface area, charge transport and recombination also affect the photovoltaic performance. To elucidate the charge transfer kinetics in DSSCs, intensity modulated photovoltage spectroscopy (IMVS) was performed to determine the electron lifetime (τ), intensity modulated photocurrent spectroscopy (IMPS) was performed to derive the time constants for determination of electron diffusion coefficients (D),[14,15] and charge extraction technique was used to extract the charge density (Q). Figure 5 compares the electron lifetimes against charge density for NP chains and separated 25-nm NPs. The logarithm of electron lifetime decreases linearly with the logarithm of charge density,[14] and the slope is similar for the two cases. At the same charge density, the electron lifetime for the NP chains is longer than that for the separated NPs by 4.5-fold. The electron diffusion coefficient for the 25-nm separated NPs obtained from the hydrothermal treatment is 2.5-fold that for the as-prepared NP chains (Figure 6). The hydrothermally treated 25-nm NPs exhibit faster electron diffusion than the 5-nm NP chains without hydrothermal treatment. This is likely because the hydrothermally treated sample has better crystallinity and lower surface area than the sol-gel product.[16]

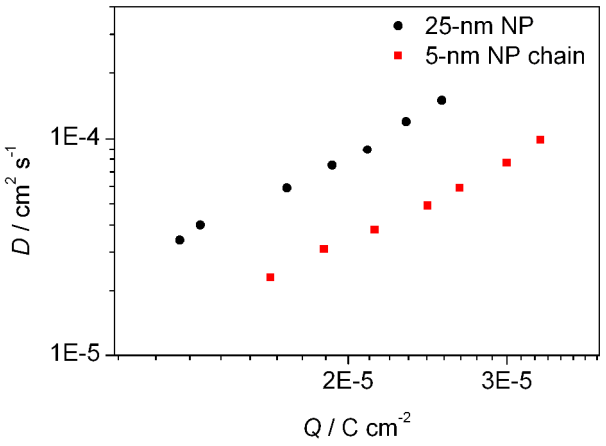

Figure 6. Electron diffusion coefficient against charge density

Despite the higher surface area offering more traps and electron acceptors for charge recombination, the electron lifetime for the NP chains is much longer than that for the separated NPs. The longer electron lifetime for the NP chains may be related to its slower electron diffusion rate.[17] In addition, the diffusion of triiodide is limited by such a small pore size.[9,11] The small pore size is very small so that triiodide ions cannot penetrate the pores effectively.[9] The surface concentration of triiodide is thus decreased due to the diffusion limitation, and the charge recombination rate is consequently lowered with the reduced surface concentration of triiodide ions.[14,16] As a result, although the NP chains have very high surface area, longer electron lifetime is observed.

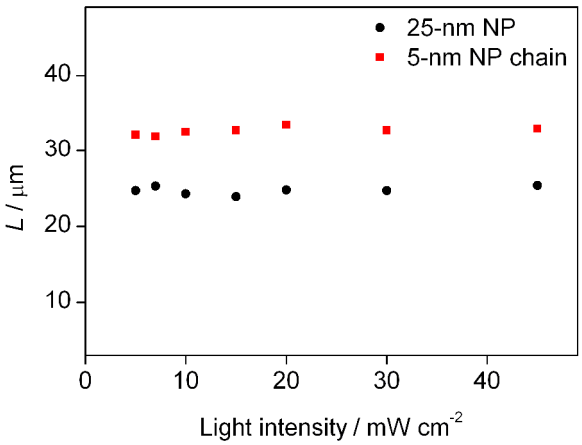

Figure 7. Comparison of electron diffusion length for 5-nm NP chains and 25-nm separated NPs.

The electron diffusion length ($L = (D \times \tau)^{1/2}$) for the NP chains is larger than that for the 25-nm NPs by more than 30% (Figure 7). This indicates that the NP chains are superior to the separated 25-nm NPs for use as photoanode of DSSCs.[18] As compared to the 25-nm separated NPs, the higher specific surface area in combination with the longer electron diffusion length for the NP chains accounts for its higher photocurrent. Owing to the high surface area, the NP chain film may be suitable for solid-state solar cell, in which a thin film is desired. The NP chains exhibit higher open-circuit photovoltage due to the larger electron lifetime along with the higher photocurrent.[14]

According to the literature,[9,10] it is difficult for NPs as small as 5 nm to achieve high efficiency. However, we obtained high efficiency using small NPs because these small NPs partially fused into long NP chains, which are not small and similar to nanorods.[10] Considering that long-thin nanorods achieve high efficiency, it is reasonable for the NP chains to yield high performance.

Conclusions

In summary, nanocrystalline anatase TiO_2 NP chains are obtained at low temperature without subsequent hydrothermal treatment. Large surface area, which enables high dye adsorption, in combination with the NP chain feature, which slows down charge recombination and enhances electron diffusion length, is responsible for the obtained high efficiency. The high surface area makes it possible for a thin film to harvest incident light efficiently, which is expected to improve efficiency significantly because a thin film is favourable for high photovoltage generation. This approach, making the preparation processes of TiO_2 much easier and safer, facilitates massive production and

offers an effective pathway for the improvement of efficiency and the reduction of cost as well.

Experimental Section

Synthesis of TiO_2 NP chains. 50 ml TTPP was added dropwise to 100 ml HAc under vigorous stirring. No precipitate was formed during this procedure. Afterwards, 300 ml water was dropwise added into the above solution within 10 min under vigorous stirring. White precipitate was formed at the beginning, which was then changed to a clear solution. The mixture, which was heated at 50 ^oC under stirring for 10 h, gradually became turbid and finally became a bluish gel. The as-prepared powder and the sintered sample at 500 ^oC for 2h were used to perform corresponding characterizations such as XRD and TEM.

DSSC Fabrication and Evaluation

Titania paste was prepared by mixing 100 mL TiO_2 solution in ethanol (10 mg cm^{-3}), 0.45 g ethyl cellulose (TCI) and 3.5 g α-terpineol (Acros) followed by removal of ethanol on a rotary evaporator at a reduced pressure. TiO_2 films (5 mm × 5 mm) composed of the as-prepared NP chains or the separated 25-nm NPs were fabricated by screen-printing the paste onto the conductive glass (F-doped SnO_2, FTO, 14 Ω per square, transmittance of 85%, Nippon Sheet Glass Co., Japan). The dye sensitizer used in this work was cis-di(isothiocyanato)-bis-(2,2-bipyridyl-4,4-dicarboxylato) ruthenium (II) bis-tetrabutyl ammonium (the so-called N719, used as received from Solaronix SA) (0.3 mM in a mixed solvent of acetonitrile and tert-butanol in a volume ratio of 1:1). Sealed DSSC devices sandwiched with the redox electrolyte (0.1 M LiI, 0.05 M I_2, 0.6 M 1,2-dimethyl-3-n-propylimidazolium iodide, and 0.5 M 4-tert-butylpyridine in anhydrous acetonitrile) were fabricated for evaluation of photovoltaic performance. A Keithley-2420 source meter in combination with a Sol3A class AAA solar simulator IEC/JIS/ASTM equipped with an AM1.5G filter and 45 W Xenon lamp was used to measure the current-voltage curves. The intensity of white light was calibrated with a reference silicon solar cell (Oriel-91150). To avoid stray light, a black mask with an aperture area of 0.2354 cm^2 was put on the surface of devices during measurements. Anti-reflection film was not used to reduce the incident light losses. Incident monochromatic photon-to-electron conversion efficiency (IPCE) as a function of wavelength was recorded on an Oriel-74125 system (Oriel Instruments). The intensity of monochromatic light was measured with a Si detector (Oriel-71640).

Characterizations. X-ray diffraction (XRD) was performed on D8 Advance (Bruker, Cu Kα radiation: λ = 0.154 nm). High-resolution transmission electron microscopy (HRTEM) was carried out on JEM-2100F (JEOL) and Tecnai G2 20 TWIN (FEI, USA). The specific surface area was measured with a Micromeritics ASAP2020 nitrogen adsorption-desorption apparatus. The UV-vis spectra were recorded on Shimadzu UV-2550 UV-vis spectrometer. An electrochemical workstation (ZAHNER ZENNIUM CIMPS-1, Germany) was used to perform intensity modulated photocurrent/photovoltage spectroscopy (IMPS/IMVS) and charge extraction under illumination of a green light emitting diode (LED, 532 nm). The intensity-modulated spectra were measured at room temperature with light intensity ranging from 0.5 to 45 W m^{-2} in modulation frequency ranging from 0.1 Hz to 10 kHz with modulation amplitude less than 5% of the light intensity.

Acknowledgment

This work was financially supported by the National Basic Research Program (No. 2011CB933302) of China, STCSM (12JC1401500) and Jiangsu Major Program (BY2010147).

Notes and references

Department of Chemistry, Collaborative Innovation Centre of Chemistry for Energy Materials, Department of Macromolecular Science, State Key Laboratory of Molecular Engineering of Polymers, Lab of Advanced Materials, Fudan University, 2205 Songhu Road, Shanghai 200438, P. R. China

* Corresponding author. E-mail: zs.wang@fudan.edu.cn

§ Electronic Supplementary Information (ESI) available: See DOI: 10.1039/b000000x/

1. B. O'Regan, M. Grätzel, *Nature* 1991, **353**, 737.
2. A. Yella, H.-W. Lee, H. N. Tsao, C. Yi, A. K. Chandiran, M. Nazeeruddin, E. W.-G. Diau, C.-Y. Yeh, S. M. Zakeeruddin, M. Grätzel, *Science* 2012, **334**, 629.
3. W.-Q. Wu, Y.-F. Xu, H.-S. Rao, C.-Y. Su, D.-B. Kuang, *J. Am. Chem. Soc.* 2014, **136**, 6437.
4. D. Chen, F. Huang, Y.-B. Cheng, R. A. Caruso, *Adv. Mater*. 2009, **21**, 2206.
5. H.-J. Koo, Y. J. Kim, Y. H. Lee, W. I. Lee, K. Kim, N.-G. Park, *Adv. Mater*. 2008, **20**, 195.
6. X. Feng, K. Zhu, A. J. Frank, *Angew. Chem. Int. Ed*. 2012, **51**, 2727.
7. Y. Kusumawati, M. Hosni, M. A. Martoprawiro, S. Cassaignon, T. Pauporté, *J. Phys. Chem. C*, 2014, **118** , 23459.
8. M. K. Nazeeruddin, A. Kay, I. Rodicio, R. Humphry-Baker, E. Müller, P. Liska, N. Vlachopoulos, M. Grätzel, *J. Am. Chem. Soc.* 1993, **115**, 6382.
9. K. Park, Q. Zhang, D. Myers, G. Cao, *ACS Appl. Mater. Interfaces* 2013, **5**, 1044.
10. W. Zhang, Y. Xie, D. Xiong, X. Zeng, Z. Li, M. Wang, Y.-B. Cheng, W. Chen, K. Yan, S. Yang, *ACS Appl. Mater. Interfaces* 2014, **6**, 9698.
11. C. J. Barbé, F. Arendse, P. Comte, M. Jirousek, F. Lenzmann, V. Shklover, M. Grätzel, *J. Am. Ceram. Soc*. 1997, **80**, 3157.
12. P. D. Cozzoli, A. Kornowski, H. Weller, *J. Am. Chem. Soc*. 2003, **125**, 14539.
13. Z.-S. Wang, H. Kawauchi, T. Kashima, H. Arakawa, *Coord. Chem. Rev*. 2004, **248**, 1381-1389.
14. G. Schlichthörl, N. G. Park, A. J. Frank, *J. Phys. Chem. B* 1999, **103**, 782.
15. A. C. Fisher, L. M. Peter, E. A. Ponomarev, A. B. Walker, K. G. U. Wijayantha, *J. Phys. Chem. B* 2000, **104**, 949.
16. S. Nakade, Y. Saito, W. Kubo, T. Kitamura, Y. Wada, S. Yanagida, *J. Phys. Chem. B* 2003, **107**, 8607.
17. N. Kopidakis, K. D. Benkstein, J. v. d. Lagemaat, A. J. Frank, *J. Phys. Chem. B* 2003, **107**, 11307.
18. L. M. Peter, *J. Phys. Chem. C* 2007, **111**, 6601.

TOC

Titania chains composed of 5 nm nanoparticles are prepared at low temperature without hydrothermal reaction for efficient dye-sensitized solar cells.